Colloid Polym Sci (2013) 291:2181–2189
DOI 10.1007/s00396-013-2957-2

ORIGINAL CONTRIBUTION

Alternating copolymerization of carbon dioxide and cyclohexene oxide catalyzed by salen Co^{III}(acetate) complexes

Yongsheng Niu · Hongchun Li

Received: 23 January 2013 / Revised: 6 April 2013 / Accepted: 11 April 2013 / Published online: 24 April 2013

Abstract A series of Co^{III} carboxylate based upon *N*,*N*,*O*,*O*-tetradentate Schiff base ligand framework have been prepared. X-ray diffraction analysis confirms that these Schiff base Co^{III} carboxylate are all monomeric species with a six-coordinated central Co in their solid structures. The activities and polycarbonate selectivity of these complexes toward the copolymerization of epoxide (cyclohexene oxide and propylene oxide) and carbon dioxide have been investigated in the presence of bis(triphenylphosphine)iminium chloride. Copolymerization experiments indicate that [bis(α-methyl-3,5-di-*tert*butyl-salicylaldehyde) ethylenediiminato] $Co^{III}OOCH_3$ exhibits the highest activity and polycarbonate selectivity among these Co^{III} carboxylate. The resultant copolymer contained almost 100 % carbonate linkages with the molecular weight up to 71.8 kg mol^{-1} as well as narrow polymer dispersity index (polymer dispersity index = 1.5). The substituents and the mode of the bridging part between the two nitrogen atoms both exert significant influences upon the progress of the copolymerizations, influencing both the polycarbonate selectivity and the rate of copolymerization.

Keywords Biodegradable · Carbon dioxide · Copolymerization · Polycarbonates · Poly(cyclohexene oxide)

Introduction

The transition metal complexes with Schiff bases as ligands are promising systems for application in the coupling of CO_2 with epoxide to aliphatic polycarbonates because the copolymerization of CO_2 and epoxide [such as cyclohexene oxide (CHO), propylene oxide (PO)] with discrete metal complex has been well documented [1]. Copolymers of CHO with CO_2 are important product with favorable property in comparison to homopoly(cyclohexene oxide), which is also one of the most promising routes for the chemical fixation of carbon dioxide [2–4]. For another, introduction of a CO_2 comonomer to the poly(cyclohexene oxide) chain changes the structure, and consequently, the properties of the polymer product are obtained. The effect is dependent on the type of catalytic system used and polymerization conditions [5].

Metal salen complexes have been used for the copolymerization of CO_2 with certain monomers to form polycarbonates [6–9]. A particular feature of these complexes is that polymers tend to be isolated with very narrow molecular weight distributions and that the molecular weights of the produced copolymer can be controlled. Typically, these complexes are tolerant toward water and air, so that extensive drying and purification of reagents are unnecessary. (Salen)$Cr^{III}X$ or (salen)$Co^{III}X$ complexes (salen=*N*,*N*′-bis(salicylidene)-1,2-diaminoalkane), which exhibit outstanding performance and can obtain the carbonate contents reach almost 100 %, are composed of zinc acetate complexes [10], tetrakis(pentafluorophenyl)porphyrin chromium(III) chloride [11] and β-diiminate zinc complexes [12, 13]. (Salen)$Cr^{III}X$ [14–18] or (Salen)$Co^{III}X$ [19–25] complexes [salen=*N*,*N*′-bis(salicylidene)-1,2-diaminoalkane] exhibit outstanding performance, and the carbonate contents reach almost 100 %. These studies should be very important for designing a highly efficient complex and for understanding the scope and the limitation of these types of transition metal complexes as CHO/CO_2 copolymerization catalysts.

Metal salen complexes have received increasing attention for their unusually high catalytic activity on the copolymerization of CO_2 with epoxide [1]. The influence of the

Y. Niu · H. Li (✉)
College of Chemistry & Pharmacy, Qingdao Agricultural University, Qingdao 266109, China
e-mail: hclichifeng@163.com

phenolate ortho and para substituents as well as the axial group epoxide/CO_2 copolymerization has been studied widely [6, 26, 27]. The cobalt Schiff base complex with axial acetate ligand has been employed to the carbon dioxide fixation field. However, some thought one cobaltate complex with one axial acetate ligand and others reported cobaltate complex with two axial acetate ligands [22, 23, 28–33]. Coates and coworkers [34] reported that a five-coordinated cobalt complex is pseudo square-pyramidal with Co located slightly above the plane of the salen ligand in the direction of the axial ligand. Recently, we reported the X-ray crystal structure of the salen Co^{III}(2,4-dinitrophenoxy) is six coordinated [35, 36]. As far as we are aware, the crystal structure of the cobalt Schiff base complexes with axial acetate ligand has not been reported.

In the present work, a series of novel α-methyl ligated $cobalt^{III}$ carboxylate Schiff bases complexes were developed to synthesis the alternating copolymer of CHO/CO_2 with an ionic quaternary ammonium salt bis(triphenylphosphine)iminium chloride [PPN]Cl as a cocatalyst. The influences of the ligand framework and the reaction conditions on the catalytic activities of the related complexes will be explicated. Based on the X-ray crystal structure and results of copolymerization of CO_2 with CHO, the copolymerization mechanism is examined as well.

Experimental section

General methods

All manipulations involving air- and/or water-sensitive compounds were carried out using standard Schlenk techniques under dry argon. CHO was refluxed over CaH_2, and fractionally distilled under an argon atmosphere prior to use. CO_2 (99.995 %) was purchased from Qingdao Institute of Special Gases and used as received. Diethyl ether was distilled from sodium benzophenone. Methylene chloride, hexane, and chloroform were distilled from CaH_2 under argon. All ligands were synthesized according to modified literature procedures [37–39].

Measurements

Nuclear magnetic resonance (NMR) spectra were recorded on a Bruker AV 300M instrument at room temperature. Chemical shifts were given in parts per million from tetramethylsilane. Gel permeation chromatography (GPC) measurements were carried out with a Waters instrument (515 HPLC pump) equipped with a Wyatt interferometric refractometer. GPC columns were eluted with THF at 25 °C at 1 ml min^{-1}. The molecular weights were calibrated against polystyrene standards. IR spectra were recorded on a Perkin-Elmer 2000 FTIR spectrometer. matrix-assisted laser desorption-ionization time-of-flight mass spectrometry (MALDI-TOF) MS analyses were carried out on a commercial Reflex III MALDI-TOF mass spectrometer (Bruker Co., Germany) equipped with delayed extraction technology. Ions formed by a pulsed UV laser beam with 3 nm pulse (nitrogen laser, λ=337 nm) were accelerated through 20 kV, and detection voltage was set at 1.60 kV. The laser was adjusted by the experiments slightly above the threshold, and the mass spectra were obtained from the results of 35 laser shots in positive mode. The matrix, trans-3-indoleacrylic acid, was dissolved in purified THF (0.1 mol l^{-1}), and the solution was mixed with the polymer solution in THF (5 mg ml^{-1}) in a 1:1 *v*/*v* ratio. Crystallographic data were collected on a Bruker APEX CCD diffractometer with graphite-monochromated Mo Kα radiation (λ=0.71073 Å) at 293 K. The structure was refined by the full-matrix least-squares method on F^2 using the SHELXTL-97 crystallographic software package. Anisotropic thermal parameters were used to refine all nonhydrogen atoms. Hydrogen atoms were located in idealized positions.

Synthesis of complexes **1**–**6**

Synthesis of complex **1** To a stirred mixture of salen Co^{II} complex (1.16 g, 2.0 mmol) in CH_2Cl_2 (150 ml), the mixture of CH_3COOH (0.12 g, 2.0 mmol, 1 equiv.) and CH_2Cl_2 (20 ml) was added. The solution was stirred under dry oxygen atmosphere at room temperature for 60 min. The solvents were removed in vacuum to leave a crude green dark solid in near 100 % yield. The resulted solid was further treated with the mixture of diethyl ether and hexane, and then dried at 60 °C in vacuum for 24 h. Yield: 89 %. Elemental analysis calcd (%) for $C_{36}H_{53}CoN_2O_4$: C, 67.90; H, 8.39; N, 4.40. Found: C, 67.87; H, 8.35; N, 4.33. ^{1}H NMR (1,4-Dioxane-*d8*): 1.12(s, 6H), 1.32 (s, 18H), 1.74 (s, 18H), 2.14 (s, 2H), 4.13 (m, 4H), 7.41 (s, 2H), 7.49 (s, 2H). ^{13}C NMR (1,4-Dioxane-*d8*): δ 19.02, 27.14, 23.57, 30.35, 31.47, 32.48, 40.71, 124.06, 121.22, 126.48, 128.98, 137.48, 142.41, 163.69, 176.27. ESIMS (*m*/*z*, M^++H): 577.3201; Calcd. for $[C_{34}H_{50}N_2O_2Co]^+$: 577.3204.

Synthesis of complex **2** It was synthesized according to the literature method [35]. Yield: 91 %. Elemental analysis calcd (%) for $C_{34}H_{49}CoN_2O_4$: C, 67.09; H, 8.11; N, 4.60. found: C, 67.05; H, 8.04; N, 4.55. ^{1}H NMR (1,4-Dioxane-*d8*): 1.31 (s, 18H), 1.73 (s, 18H), 2.09 (s, 3H), 4.12 (m, 4H), 7.39 (s, 2H), 7.45 (s, 2H). 8.12 (s, 2H). ^{13}C NMR (1,4-Dioxane-*d8*): δ 24.56, 30.75, 30.27, 31.48, 33.49, 58.25, 122.16, 125.42, 127.37, 137.72, 142.41, 151.35, 162.69, 168.70. ESIMS (*m*/*z*, M^+ + H): 549.2890; Calcd. for $[C_{32}H_{46}N_2O_2Co]^+$: 549.2891.

Synthesis of complex **3** It was synthesized as a similar procedure of complex **1**. Yield: 85 %. Elemental analysis calcd (%) for $C_{28}H_{35}CoI_2N_2O_4$: C, 43.32; H, 4.54; N, 3.61; found: C, 43.28; H, 4.51; N, 3.60. ^{1}H NMR (1,4-Dioxane-*d8*): 1.10 (s, 6H), 1.37 (s, 18H), 2.09 (s, 3H), 4.02 (m, 4H), 7.49 (s, 2H), 7.55 (s, 2H). ^{13}C NMR (1,4-Dioxane-*d8*): δ 20.56, 29.67, 30.15, 32.17, 125.16, 128.42, 138.37, 137.12, 151.35, 163.59, 169.71. ESIMS (*m*/*z*, M^++H): 716.9882; Calcd. for $[C_{26}H_{32}I_2N_2O_2Co]^+$: 716.9885.

Synthesis of complex **4** It was synthesized as a similar procedure of complex **1**. Yield: 88 %. Elemental analysis calcd (%) for $C_{28}H_{35}CoI_2N_2O_4$: C, 43.32; H, 4.54; N, 3.61; found: C, 43.29; H, 4.50; N, 3.59. ^{1}H NMR (1,4-Dioxane-*d8*): 1.06 (s, 6H), 1.31 (s, 18H), 2.07 (s, 3H), 4.05 (m, 4H), 7.45 (s, 2H), 7.51 (s, 2H). ^{13}C NMR (1,4-Dioxane-*d8*): δ 20.16, 25.63, 30.25, 31.45,40.15, 89.16, 125.92, 126.37, 139.98, 144.34, 1631.35, 164.59, 169.78. ESIMS (*m*/*z*, M^++H): 716.9880; Calcd. for $[C_{26}H_{32}I_2N_2O_2Co]^+$: 716.9885.

Synthesis of complex **5** It was synthesized as a similar procedure of complex **1**. Yield: 87 %. Elemental analysis calcd (%) for $C_{20}H_{17}CoI_4N_2O_4$: C, 26.23; H, 1.87; N, 3.06. found: C, 26.20; H, 1.85; N, 3.07. ^{1}H NMR (1,4-Dioxane-*d8*): 1.08 (s, 6H), 2.09 (s, 3H), 4.07 (m, 4H), 7.76 (s, 2H), 7.79 (s, 2H). ^{13}C NMR (1,4-Dioxane-*d8*): δ 21.34, 24.63, 29.24, 89.16, 91.21, 128.12, 136.37, 139.98, 147.74, 1661.31, 165.59, 169.89. ESIMS (*m*/*z*, M^++H): 856.6564; Calcd. for $[C_{18}H_{14}I_4N_2O_2Co]^+$: 856.6566.

Synthesis of complex **6** It was synthesized according to the literature method [35]. Yield: 89 %. Elemental analysis calcd (%) for $C_{37}H_{55}CoN_2O_4$: C, 68.29; H, 8.52; N, 4.30; found: C, 67.32; H, 8.67; N, 4.51. ^{1}H NMR (1,4-Dioxane-*d8*): 1.35 (s, 18H), 1.37 (s, 18H), , 1.65 (s, 6H), 2.09 (s, 3H), 7.64 (s, 2H), 7.69 (s, 2H). ^{13}C NMR (1,4-Dioxane-*d8*): δ 24.54, 30.13, 31.25, 32.46, 31.66, 62.71, 128.12, 128.56, 137.37, 139.88, 145.94, 154.54, 164.37, 170.45. ESIMS (*m*/*z*, M^++H): 591.3363; Calcd. for $[C_{35}H_{52}N_2O_2Co]^+$: 591.3361.

Representative copolymerization procedure

A 100-ml stainless steel autoclave equipped with a magnetic stirring bar was heated to 120 °C under vacuum for 2 h. After cooled to room temperature, the autoclave was charged with CO_2. A mixture of complex and [PPN]Cl was dissolved in 1,4-dioxane under CO_2 atmosphere. The mixture solution was injected into the autoclave with a syringe under CO_2 atmosphere, followed by the addition of CHO. The autoclave was heated to a desired temperature in an oil bath and the 1.5 MPa pressure of CO_2. The mixture was stirred for the allotted reaction time, then quickly cooled to room temperature and vented in a fume hood. A small aliquot of the resultant copolymerization mixture was removed from the reactor for ^{1}H NMR analysis. The remaining copolymerization mixture was then dissolved in chloroform, quenched with 5 % HCl solution in methanol, and precipitated from methanol. The copolymer was collected and dried in vacuum to constant weight, and the copolymer yield was determined. The carbonate linkages were determined from the relative intensity of the cyclohexyl methine proton signals (4.6 ppm for carbonate linkages and 3.4 ppm for ether linkages) in the ^{1}H NMR spectrum of the polymer. The molar mass and the molar mass distribution of the resulting polymer were determined by GPC.

Results and discussion

Syntheses of complexes

Substituted derivatives of the parent ligand salen were prepared by condensation of salicylaldehyde derivatives with ethylenediamine. Substituted salicylaldehydes were prepared via the Reimer–Tiemann reaction or through lithium aluminum hydride reduction followed by manganese dioxide oxidation of a substituted salicylic acid [37–39]. Stirring the Schiff base ligands with cobalt^{II} acetate tetrahydrate under aerobic conditions afforded the requisite Co^{III} complexes [38]. The nature of the R_1, R_2, and R_3 substituents, the hydrocarbonated chain R, and their abbreviations are also shown in Fig. 1.

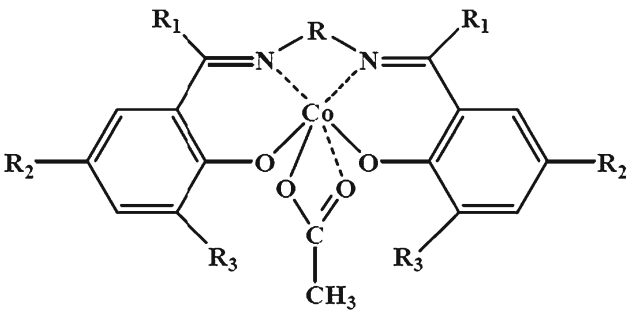

Complex	R_1	R_2	R_3	R
1	CH_3	^{t}Bu	^{t}Bu	$(CH_2)_2$
2	H	^{t}Bu	^{t}Bu	$(CH_2)_2$
3	CH_3	I	^{t}Bu	$(CH_2)_2$
4	CH_3	^{t}Bu	I	$(CH_2)_2$
5	CH_3	I	I	$(CH_2)_2$
6	H	^{t}Bu	^{t}Bu	$CH_2C(CH_3)_2CH_2$

Fig. 1 Salen Co^{III} acetate complexes for cyclohexene oxide/CO_2 copolymerization

The product was sufficiently dried under reduced pressure. Complexes **1**–**6** were isolated as a solid powder. Numerous attempts to isolate complexes **1**–**5** in a mixture of methylene chloride and hexane or other solvents were proved to be unsuccessful. Fortunately, the structure of a closely related complex **6** could be elucidated by single crystal X-ray analysis. Crystal suitable for X-ray diffraction was grown from a mixture of methylene chloride and hexane at 20 °C. A single crystal was selected for X-ray analysis (Table 1). As shown in Fig. 2, the structure is indeed a six-coordinate octahedral as the structure of the salen Co^{III}(2,4-dinitrophenoxy) [35, 36]. X-ray diffraction data showed that the crystal was analogous monomeric structures. The overall geometry around the metal cobalt was a six-coordinate octahedral with an average compressed axial O(2)–Co(1)–O(3) bond angle of 167.20(9)°, and equatorial O(1)–Co(1)–N(1), N(1)–Co(1)–N(2), O(2)–Co(1)–O(4), and O(4)–Co(1)–O(1) bond angles of 91.22(9)°, 92.17(10)°, 100.69(9)°, and 86.57(9)°, respectively. The distances from the Co atom to O(1), O(2), O(3), O(4), N(1), and N(2) were 1.871(2), 1.871(2), 1.962(2), 1.988(2), 1.880(2), and 1.899(3) Å, respectively (Table 2). The average Co–N and Co–O bond lengths are in the same range as corresponding values in similar octahedral Co^{III} systems [40, 41]. The molecular structure of complex **6** is shown in Fig. 2.

Table 1 Crystal data and structure refinement parameters for complex **6**

Empirical formula	$C_{37}H_{55}CoN_2O_4$
Formula weight	650.76
Temperature (K)	293(2)
Wavelength (Å)	0.71073
Crystal system	Monoclinic
Space group	C2/c
Unit cell dimensions	
a (Å)	25.197(3)
b (Å)	14.7486(17)
c (Å)	23.101(3)
α (°)	90
β (°)	108.344(2)
γ (°)	90
Volume ($Å^3$)	8148.8(16)
Z	8
Calculated density(Mg m^{-3})	1.061
Absorption coefficient (mm^{-1})	0.455
F (000)	2,800
Crystal size (mm)	0.48×0.18×0.13
Theta range for data collection (°)	1.62–25.39
Limiting indices (*hkl* range)	$-30\le h\le 19$, $-17\le k\le 17$, $-26\le l\le 27$
Reflections collected	21,475
Independent reflections	7,465
R_{int}	0.0380
Data/restraints/parameters	7,465/0/412
Goodness-of-fit on F^2	1.024
Final *R* indices [$I>2\sigma(I)$]	R_1=0.0593, wR_2=0.1619
R indices (all data)	R_1=0.0815, wR_2=0.1752
Largest difference in peak and hole (e $Å^{-3}$)	0.542 and −0.274

Copolymerization of CHO and CO_2

Different Co^{III} complexes were evaluated as catalysts for the copolymerization of CHO and CO_2 in the presence of [PPN]Cl under various reaction conditions. These complexes exhibit different catalytic activities. As shown in Table 3, complex **1** bearing ligand with the R_1 being a donor electronic methyl group displays the highest catalytic activity (see entry 1, in Table 3). The reason that the catalytic activity depended on the structure of ligand should be attributed to that donor electronic methyl could stabilize the active salen Co^{III} species against decomposition to inactive salen Co^{II} by reversibly intramolecular Co–O bond formation and dissociation. When the R_2 or R_3 group is replaced by an iodine atom, complexes **3** and **5** present a moderate catalytic activity (see entries 3 and 5, in Table 3). Complex **6** bearing the sterically less bulky ligands shows the lowest activity among its analogues complexes **1**–**6**. Under the same conditions, when the R_1 group is replaced by a hydrogen atom, complex **2** exhibits a lower catalytic activity (see entry 2, in Table 3). While diimine-bridges with the two carbon atoms are superseded by that with the three carbon atoms, the catalytic activity is dramatically decreased. The catalytic activity is influenced markedly by the nature of the substituents grafted on the ligands molecules and the length of the diimine bridges between the two nitrogen atoms in the ligands, respectively. These results might be mainly ascribed to the steric bulk effect of the substituents R on the phenolates of the ligand. This agrees well with the literature data [5]. These differences in ligands framework and the length of the diimine bridges between the two nitrogen atoms in the ligands also reflect on the selectivity formation of poly(cyclohexenylene carbonate) (PCHC) over cyclohexene carbonate (CHC) and the resulting copolymer number average molecular weights (M_n). Complex **1** displays the highest PCHC/CHC selectivity and yields polymer with the highest M_n. However, complex **6** presents the lowest PCHC/CHC selectivity and produces polymer with the lowest M_n. Both the length of the diimine bridges and the substituents on the ligands do not have a clear effect on the microstructure of the resultant polymer. With complexes **1**–**6** the copolymerization afford products possessing >99 % carbonate linkages.

The mole ratio of [PPN]Cl to the complex **1** played an important role in the copolymerization of CHO with CO_2, as

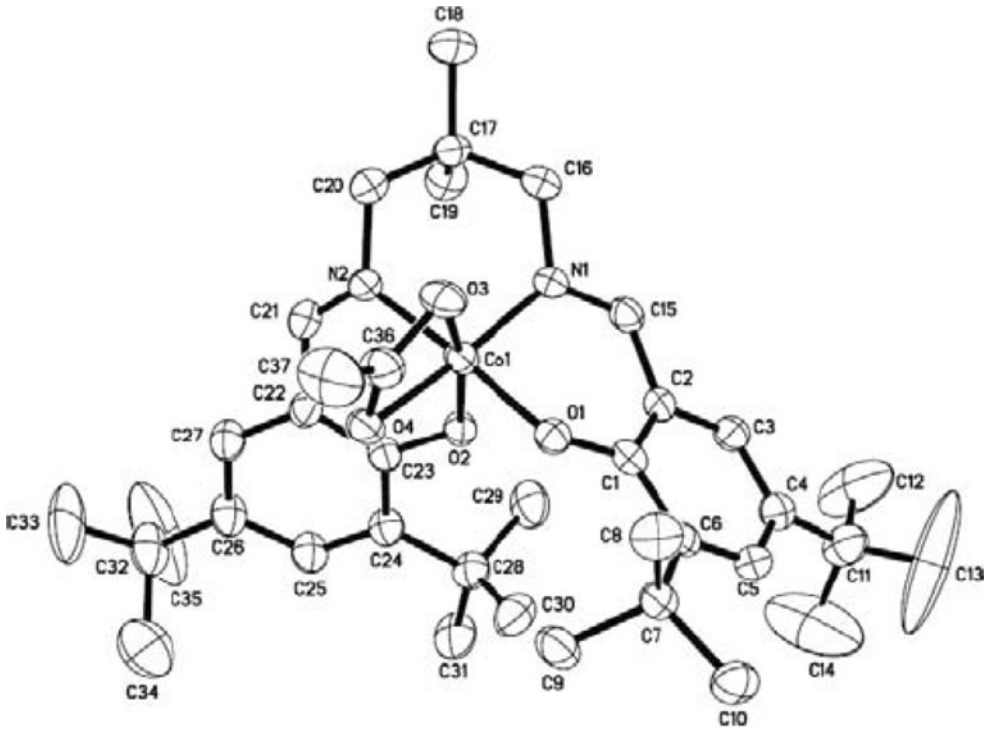

Fig. 2 Molecular structure of complex **6**

Table 2 Selected bond distances (Å) and angles (°) for complex **6**

Co–N(1)	1.880(2)
Co–N(2)	1.899(3)
Co–O(2)	1.871(2)
Co–O(1)	1.871(2)
Co–O(3)	1.962(2)
Co–O(4)	1.988(2)
O(1)–Co(1)–O(2)	90.41(9)
O(2)–Co(1)–N(1)	91.55(9)
O(2)–Co(1)–N(2)	90.67(10)
O(1)–Co(1)–O(3)	87.85(10)
N(1)–Co(1)–O(3)	101.16(10)
O(1)–Co(1)–O(4)	86.57(9)
N(1)–Co(1)–O(4)	167.57(10)
O(3)–Co(1)–O(4)	66.56(9)
O(2)–Co(1)–C(36)	133.55(11)
N(2)–Co(1)–C(36)	91.37(12)
O(4)–Co(1)–C(36)	32.93(10)
O(1)–Co(1)–N(1)	91.22(9)
O(1)–Co(1)–N(2)	176.42(9)
N(1)–Co(1)–N(2)	92.17(10)
O(2)–Co(1)–O(3)	167.20(9)
N(2)–Co(1)–O(3)	90.35(10)
O(2)–Co(1)–O(4)	100.69(9)
N(2)–Co(1)–O(4)	89.87(10)
O(1)–Co(1)–C(36)	85.41(11)
N(1)–Co(1)–C(36)	134.70(12)
O(3)–Co(1)–C(36)	33.67(10)

listed in Table 4 (entries 1–4). Although almost negligible yield was observed in the absence of cocatalyst (see entry 1 in Table 4), the addition of cocatalyst [PPN]Cl resulted in the production of the alternating copolymer (see entries 2–4, in Table 4). Optimization of the molar ratio between complex **1** and [PPN]Cl revealed that the highest yield was achieved using 1 equiv. of [PPN]Cl. However, the increase in the ratio of [PPN]Cl to complex **1** above 2 equiv. could increase the reaction activities. The CHC only was obtained. The CHC formation might be based on the presence of a depolymerization reaction that is promoted at higher [PPN]Cl concentrations. It is most likely due to a backbiting reaction starting from an alcoholate chain end that is displaced from the Co^{III} center in a coordination equilibrium with [PPN]Cl after epoxide ring opening [18].

The influence of reaction temperature on the copolymerization of CHO and CO_2 was investigated using complex **1**/[PPN]Cl (see entries 3 and 5–7, in Table 4). Dramatic increase in catalytic activity with temperature was observed, and the turnover frequency (TOF) at 80 °C (48.7 h^{-1}) almost doubles that at 60 °C (25.6 h^{-1}) (see entries 3 and 5, in Table 4), which reaches to 52.2 h^{-1} when the copolymerization is performed at 100 °C (see entry 6, in Table 4). The highest catalytic activity (54.5 h^{-1}) is achieved at 120 °C (see Entry 7, in Table 4). While the yield of copolymer increases with increasing temperature up to about 80 °C, and then decreases with the further increase. Similar results have been observed previously [33]. In agreement with the increase in yield, M_n of the obtained copolymer increases

Table 3 Copolymerization of CHO and CO_2

Entry	Complex	[CHO]/[Cat]	Time (h)	[CHO] (mol l^{-1})	Temperature (°C)	Yield[a]	TOF[b] (h^{-1})	Selectivity[c] (% PPC)	M_n[d] (kg mol^{-1})	PDI[d]
1	**1**	1,000	10	50	60	25.6	25.6	>99	21.6	1.2
2	**2**	1,000	10	50	60	10.4	12.2	85	9.3	1.4
3	**3**	1,000	10	50	60	17.0	17.5	97	14.4	1.2
4	**4**	1,000	10	50	60	18.9	19.7	96	17.1	1.2
5	**5**	1,000	10	50	60	15.8	16.6	95	14.5	1.3
6	**6**	1,000	10	50	60	0.44	2.2	20	2.1	1.5

Copolymerizations run in neat cyclohexene oxide (CHO) with [Co]/[[PPN]Cl]=1:1 at 1.5 MPa of CO_2 in 1,4-dioxane (7 ml)

[a] Based on isolated poly(cyclohexene carbonate) yield

[b] Turnover frequency: mol CHO mol Co^{-1} h^{-1}

[c] Determined by ^{1}H NMR spectroscopy ($CDCl_3$, 300 MHz)

[d] Determined by gel permeation chromatography calibrated with polystyrene standards in tetrahydrofuran at 40 °C

correspondingly from 21.6 kg mol^{-1} at 60 °C to 38.7 kg mol^{-1} at 80 °C. In the meantime, polymer dispersity index remains narrow and almost constant (PDI=1.2). It is generally known that the homopolymerization of CHO easily takes place at elevated temperatures and is normally observed at catalyst systems with regard to much-studied zinc complexes [10]. Moreover, the polycarbonates obtained at the range of 60–120 °C all have >99 % carbonate linkages.

Obviously, the mole ratio of monomer to complex plays an important role on the TOF of copolymerization, as listed in Table 4 (entries 3 and 8–10). For example, in the experiment of entry 3, TOF (10 h) is 48.7 h^{-1} when 1,000 equiv. of CHO are used. As the ratio of CHO to complex **1** decreases to 200 equiv. in entry 8, the reaction activity decreases by almost thrice, compared with entry 3. Meanwhile, PDI also slightly decreases from 1.2 to 1.1,

Table 4 Copolymerization of CHO and CO_2[a]

Entry	[PPN]Cl/complex **1**	[CHO]/[complex **1**]	Time (h)	[CHO] (mol l^{-1})	Temperature (°C)	Yield[b]	TOF[c] (h^{-1})	Selectivity[d] (% PPC)	M_n[e] (kg mol^{-1})	PDI[e]
1	0	1,000	10	50	80	Trace	–	–	–	–
2	0.5	1,000	10	50	80	10.4	12.2	99	10.3	1.2
3	1	1,000	10	50	80	48.2	48.7	99	38.7	1.2
4	2	1,000	10	50	80	Trace	—	—	—	—
5	1	1,000	10	50	60	25.6	25.6	>99	21.6	1.2
6	1	1,000	10	50	100	48.0	52.2	92	37.1	1.4
7	1	1,000	10	50	120	46.3	54.5	85	33.9	1.5
8	1	200	10	50	80	85.6	17.3	99	14.9	1.1
9	1	800	10	50	80	56.7	45.8	99	35.6	1.2
10	1	1,200	10	50	80	39.4	47.8	99	37.7	1.2
11	1	1,000	10	30	80	27.4	27.7	99	23.1	1.3
12	1	1,000	10	40	80	39.6	40.2	99	30.1	1.2
13	1	1,000	10	60	80	43.9	46.2	95	35.7	1.3
14	1	1,000	5	50	80	29.2	58.4	99	23.8	1.2
15	1	1,000	20	50	80	70.7	36.1	98	57.8	1.3
16	1	1,000	40	50	80	85.2	22.2	96	71.8	1.5

[a] Copolymerizations run in neat cyclohexene oxide (CHO) with [Co]/[PPNCl]=1:1 at 1.5 MPa of CO_2 in 1,4-dioxane (7 ml)

[b] Based on isolated poly(cyclohexene carbonate) yield

[c] Turnover frequency: mol CHO mol Co^{-1} h^{-1}

[d] Determined by ^{1}H NMR spectroscopy ($CDCl_3$, 300 MHz)

[e] Determined by gel permeation chromatography calibrated with polystyrene standards in tetrahydrofuran at 40 °C

and M_n decreases significantly from 38.7 to 14.9 kg mol^{-1}. However, the further increases in the ratio of CHO to complex **1** above 1,000 equiv. could reduce the reaction activities (see entries 3 and 10, in Table 3). Especially, when over 1,000 equiv. of CHO are selected, both drops in catalytic activity and yield of the resultant product are observed (entry 10), which could be attributed to the lowing of the catalytic concentration when overloading monomer.

Besides operation temperature and ratio of monomer to complex, initial CHO concentration is another important issue for the reaction. In our results, it is observed that the catalytic activity increases as the initial CHO concentration increases from 30 to 50 mol l^{-1} (see entries 3, 11, and 12, in Table 4) and decreases then with the further increase in CHO concentration (entry 13 in Table 4). The prolonged reaction does not lead to an observable decrease in selectivity for PCHC formation, which can be explained by the so-called solvent effect. A similar solvent effect was reported for the copolymerization with binary catalyst systems [32, 42].

^{13}C NMR spectroscopy has been extensively used to investigate CHO incorporation into polymer backbones, which can be used to estimate the tacticity of the copolymer [2, 14]. Figure 3 presents a ^{13}C NMR spectrum of the PCHC (entry 3 in Table 4). The spectrum is very similar to those of PCHC prepared with (salen)CoX catalysts [5]. Clearly, the carbonyl regions at δ=153.80–153.66 and 153.25–153.30 ppm can be assigned to the isotactic and syndiotactic structures of the PCHC chain, respectively [2]. The peaks at 153.25–153.30 ppm are assigned to the central carbonyl carbons of *r*-centered tetrads, whereas the peaks at 153.80–153.66 ppm are attributed to the central carbonyl carbons of *m*-centered tetrads [2, 14]. PCHCs revealed a strong contribution correlating to *r*-centered tetrads (78 %), indicative of syndiotactic PCHC.

MALDI-TOF mass spectrometry is specifically suitable for structural and end-group analysis [5]. Figure 4 displays a spectrum of the resultant PCHC obtained (entry 3 in Table 4). At least two series of signals with regular repeat intervals (repeating units of 142.2 mass units) were observed in the mass spectra. For the first series of peaks at

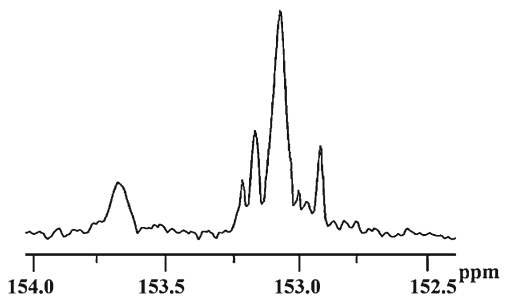

Fig. 3 Carbonyl region of the ^{13}C NMR spectrum ($CDCl_3$, 125 MHz) of PCHC from the copolymerization of CO_2/CHO sample (entry 2 in Table 4)

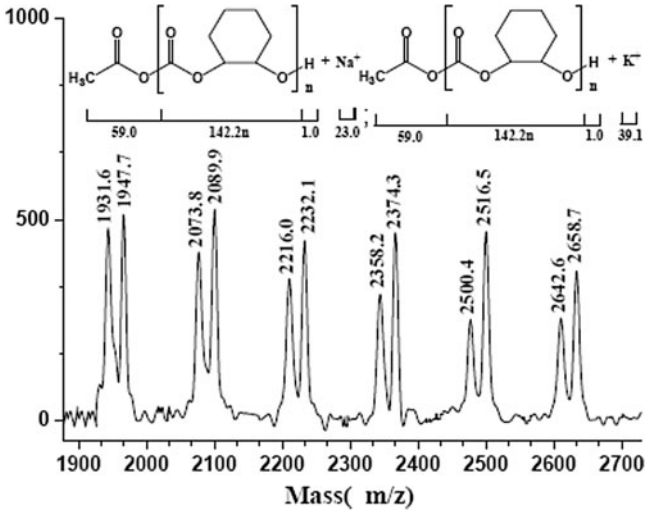

Fig. 4 MALDI-TOF mass spectrum of PCHC from the alternating copolymerization of CO_2/CHO sample (entry 2 in Table 4). mass$(m/z) = M_{CH_3COO} + nM_{repeating} + M_{Na^+}$ or mass$(m/z) = M_{CH_3COO} + nM_{repeating} + M_{K^+}$ (where $M_{CH_3OO} = 59.0$, $M_{repeating} = 142.2$ $M_{Na^+} = 23$, $M_{K^+} = 39$

the *m*/*z* of 1,931.6, 2,073.8, 2,216.0, 2,358.2, 2,500.4, and 2,642.6, there was a difference of 142.2 in *m*/*z* between every two neighboring peaks, which was also seen in the second series at the *m*/*z* of 1,947.7, 2,089.9, 2,232.1, 2,374.3, 2,516.5, and 2,658.7. Moreover, in the second series peaks in *m*/*z* were correspondingly 16 larger than those in the first series. Additionally, the weight number of propylene carbonate unit is 142.2. Thus, it could be known by calculation that the first series peaks resulted from the copolymerization reaction was initiated by insertion of CHO into a Co-acetate bond of the catalytic species attached to a Co center, and terminated with acetate groups and Na^+ ions, and K^+ ions instead of Na^+ ions for the second series.

On the basis of the information presented so far, some proposed mechanism illustrated that the monomer was inserted to the cobalt–oxygen bond of the propagating end, as shown in Scheme 1. [PPN]Cl coordinated to the metal center in the axial site transferred to the propagating metal–polymer chain, thereby labilizing the metal alkoxide bond and facilitating the insertion of CO_2 [3, 6, 17, 18, 21, 24]. The CHO monomer might be first favorably inserted into the Co–OR bond of the Schiff base cobalt complex, followed by the insertion of the CO_2 monomer. Subsequent alternating copolymerization of CHO and CO_2 affords the alternating repeating unit structure to yield the polycarbonate. The side reaction to yield the cyclic carbonate could take place through the backbiting degradation of the growing polymer–catalyst complex, which may lead to the lower polymer yield. A mechanism similar to that proposed by Darensbourg and Yarbrough using chromium salen and N-MeIm in the copolymerization of CO_2 and cyclohexene oxide [14].

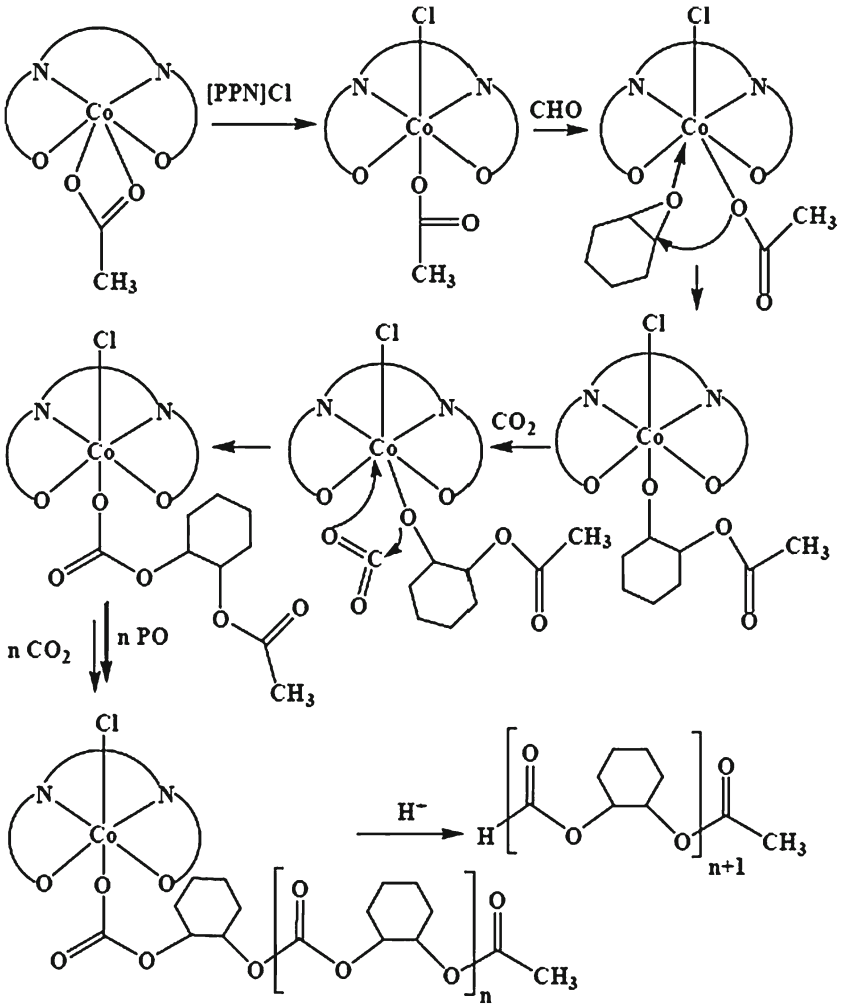

Scheme 1 Proposed mechanism for the alternating copolymerization of CO_2/CHO by complex **1** in the presence of bis(triphenylphosphine)iminium chloride

Copolymerization of PO and CO_2

By use of complex **1** and [PPN]Cl catalyst system, the copolymerization of CO_2 and PO ($[PO]_0/[[PPN]Cl]_0/[\text{complex } \mathbf{1}]_0$= 500/1/1) selectively gave the alternating copolymer in 1,4-dioxane at 60 °C in 24 h (carbonate linkages=99 %, polycarbonate/cyclic carbonate=99/1, M_n=6,400, M_w/M_n= 1.21; Table 5, run 2), although the reaction proceeded rather slowly (36.8 % yield). Also at 80 °C, the copolymeriation proceeded more rapidly to attain 42.1 % polymer yield in the same reaction time, slightly lowering the selectivity (carbonate linkages=95.8 %, polycarbonate/cyclic carbonate=92/8, M_n=7,800, M_w/M_n=1.31; Table 5, run 3). When the copolymerization was conducted at an elevated temperature, such as

Table 5 Copolymerization of PO and CO_2

Entry	Temperature (°C)	Time (h)	Yield[a]	Selectivity[b] (% PPC)	M_n[c] (kg mol^{-1})	PDI[c]
1	40	24	17.7	99	5.3	1.12
2	60	24	22.8	99	6.4	1.21
3	80	24	42.1	92	7.8	1.31
4	100	24	16.7	30	6.9	1.52
5	60	48	76.7	93	13.9	1.26

The reaction was performed in neat PO (14 ml, 200 mmol; $[PO]_0/[[PPN]Cl]_0/[\text{complex } \mathbf{1}]_0$=500:1:1) in a 100-ml autoclave at 1.6 MPa of CO_2 in in 1,4-dioxane (5 ml)

[a] Based on isolated poly(propylene carbonate) yield

[b] Determined by ^{1}H NMR spectroscopy ($CDCl_3$, 300 MHz)

[c] Determined by gel permeation chromatography calibrated with polystyrene standards in tetrahydrofuran at 40 °C

100 °C, a significant amount of cyclic carbonate (polycarbonate/cyclic carbonate=30/70) was generated under otherwise similar conditions (Table 5, run 3).

The high selectivity of polycarbonate over cyclic carbonate at 60 °C was maintained after a longer reaction time to attain quantitative formation of the alternating copolymer. The alternating copolymeriation of CO_2 and PO by using complex **1** and [PPN]Cl catalyst system was carried out at 60 °C for 48 h and afforded the alternating copolymer almost quantitatively (polycarbonate/ cyclic carbonate= 93/7, carbonate linkages=99 %, M_n=13,900, M_w/M_n= 1.26, Table 5, run 5).

Conclusions

In summary, a series of cobalt/Schiff base complexes **1**–**6** were investigated for the alternating copolymerization of CO_2 with epoxide (CHO and PO) to afford completely alternating polycarbonates with good activity in presence of [PPN]Cl. The resultant polymer has high molecular weight and high carbonate linkages as well as narrow molar mass distribution. The molecular weight of the copolymers is also sensitive to the concentration of CHO in the feed for the complexes. In addition, the solid-state structure of complex **6** was characterized, providing valuable information about the mechanism of the catalytic polymerization reaction. This strategy allows considerable scope for ligand modification and thus might lead to the design of new, efficient, and practical catalysts for the copolymerization of epoxides with CO_2.

Acknowledgment Gratitude is expressed to the Young Scientists Fund of the National Natural Science Foundation of China (grant no. 51003051), Science-Technology Foundation for Middle-Aged and Young Scientist of Shandong Province, China (grant no. BS2011CL021), and the High-level Talent Initial Funding for Scientific Research of Qingdao Agricultural University (grant no. 630924) for financial support.

References

1. Darensbourg DJ (2007) Chem Rev 107:2388–2410
2. Nakano K, Nozaki K, Hiyama T (2001) Macromolecules 34:6325–6332
3. Nozaki K, Nakano K, Hiyama T (1999) J Am Chem Soc 121:11008–11009
4. Koinuma H (2007) React Funct Polym 67:1129–1136
5. Cohen CT, Thomas CM, Peretti KL, Lobkovsky EB, Coates GW (2006) Dalton Trans 1:237–249
6. Nakano K, Kobayashi K, Nozaki K (2011) J Am Chem Soc 133:10720–10723
7. Super M, Berluche E, Costello C, Beckman E (1997) Macromolecules 30:368–372
8. Sugimoto H, Ogawa A (2007) React Funct Polym 67:1277–1283
9. Atsushi O (2010) Chem Lett 39:1066–1068
10. Kim I, Kim SM, Ha CS, Park DW (2004) Macromol Rapid Commun 25:888–893
11. Mang S, Cooper AIM, Colclough E, Chauhan N, Holmes AB (2000) Macromolecules 33:303–308
12. Cheng M, Moore DR, Reczek JJ, Chamberlain BM, Lobkovsky EB, Coates GW (2001) J Am Chem Soc 123:8738–8749
13. Moore DR, Cheng M, Lobkovsky EB, Coates GW (2003) J Am Chem Soc 125:11911–11924
14. Darensbourg DJ, Yarbrough JC (2002) J Am Chem Soc 124:6335–6342
15. Paddock RL, Nguyen ST (2001) J Am Chem Soc 123:11498–11499
16. Darensbourg DJ, Mackiewicz RM, Rodgers JL, Fang CC, Billodeaux DB, Reibenspies JH (2004) Inorg Chem 43:6024–6034
17. Nakano K, Nakamura M, Nozaki K (2009) Macromolecules 42:6972–6980
18. Darensbourg DJ, Ulusoy M, Karroonnirum O, Poland RR, Reibenspies JH, Cetinkaya B (2009) Macromolecules 42:6992–6998
19. Shi L, Lu XB, Zhang R, Peng XJ, Zhang CQ, Li JF, Peng XM (2006) Macromolecules 39:5679–5685
20. Liu BY, Gao YH, Zhao X, Yan WD, Wang XH (2010) J Polym Sci Part A: Polym Chem 48:359–365
21. Rao DY, Li B, Zhang R, Wang H, Lu XB (2009) Inorg Chem 48:2830–2836
22. Seong JE, Na SJ, Cyriac A, Kim BW, Lee BY (2010) Macromolecules 43:903–908
23. Ren WM, Zhang X, Liu Y, Li JF, Wang H, Lu XB (2010) Macromolecules 43:1396–1402
24. Noh EK, Na SJ, Kim SW, Lee BY (2007) J Am Chem Soc 129:8082–8083
25. Lu XB, Darensbourg D (2012) J Chem Soc Rev 41:1462–1484
26. Lu XB, Wang Y (2004) Angew Chem Int Ed 43:3574–3577
27. Niu YS, Zhang WX, Li HC, Chen XS, Sun JR, Zhuang XL, Jing XB (2009) Polymer 50:441–446
28. Qin Z, Thomas CM, Lee S, Coates GW (2003) Angew Chem Int Ed Engl 42:5484–5487
29. Nakano K, Kamada T, Nozaki K (2006) Angew Chem Int Ed 45:7274–7277
30. Cohen CT, Chu T, Coates GW (2005) J Am Chem Soc 127:10869–10878
31. Lu XB, Lei S, Wang YM, Zhang R, Zhang YJ, Peng XJ, Zhang ZC, Li B (2006) J Am Chem Soc 128:1664–1674
32. Cohen CT, Coates GW (2006) J Polym Sci A Polym Chem 44:5182–5191
33. Niu YS, Zhang WX, Pan X, Chen XS, Zhuang XL, Jing XB (2007) J Polym Sci A Polym Chem 45:5050–5056
34. Paddock RL, Hiyama Y, McKay JM, Nguyen ST (2004) Tetrahedron Lett 45:2023–2026
35. Niu YS, Li HC, Chen XS, Zhang WX, Zhuang XL, Jing XB (2009) Macromol Chem Phys 210:1224–1229
36. Zhuang XL, Oyaizu K, Niu YS, Koshika K, Chen XS, Nishide H (2010) Macromol Chem Phys 211:669–679
37. Postmus CJ, Kaye IA, Craig CA, Matthews RS (1964) J Org Chem 29:2693–2698
38. Ren WM, Liu Y, Wu GP, Liu J, Lu XB (2011) J Polym Sci A Polym Chem 49:4894–4901
39. Wisniewski M, Le BA, Spassky N (1997) Macromol Chem Phys 198:1227–1238
40. Ware DC, Denny WA, Clark GR (1997) Acta Crystallogr Sect C 53:1058–1059
41. Weiss MC, Bursten BB, Peng SM, Goedken VL (1976) J Am Chem Soc 98:8021–8031
42. Sugimoto H, Ohtsuka H, Inoue S (2005) J Polym Sci A Polym Chem 43:4172–4186